ARTICLES

Femtosecond Dynamics after Ionization: 2-Phenylethyl-*N*,*N*-dimethylamine as a Model System for Nonresonant Downhill Charge Transfer in Peptides

L. Lehr,[†,‡] T. Horneff,[†] R. Weinkauf,*[,§] and E. W. Schlag[†]

Institut für Physikalische und Theoretische Chemie, TU München, Lichtenbergstrasse 4, 85747 Garching, Germany, and Institut für Physikalische Chemie Heinrich-Heine-Universität, Universitätsstrasse 1, 40225 Düsseldorf, Germany

Received: May 1, 2002; In Final Form: July 5, 2005

The cation of 2-phenylethyl-*N*,*N*-dimethylamine (PENNA) offers two local sites for the charge: the amine group and 0.7 eV higher in energy the phenyl chromophore. In this paper, we investigate the dynamics of the charge transfer (CT) from the phenyl to the amine site. We present a femtosecond resonant two-color photoionization spectrum which shows that the femtosecond pump laser pulse is resonant in the phenyl chromophore. As shown previously with resonant wavelengths the aromatic phenyl chromophore can be then selectively ionized. Because the state "charge in the phenyl chromophore" is the first excited state in the PENNA cation, it can relax to the lower-energetic state "charge in the amine site". To follow this CT dynamics, femtosecond probe photoabsorption of green light (vis) is used. The vis light is absorbed by the charged phenyl chromophore, but not by the neutral phenyl and the neutral or cationic amine group. Thus, the absorption of vis photons of the probe laser pulse is switched off by the CT process. For detection of the resonant absorption of two or more vis photons in the cation the intensity of a fragmentation channel is monitored which opens only at high internal energy. The CT dynamics in PENNA cations has a time constant of 80 ± 28 fs and is therefore not a purely electronic process. Because of its structural similarity to phenylalanine, PENNA is a model system for a downhill charge transfer in peptide cations.

I. Introduction

Radical anions or cations are strongly stabilized in polar solvents. They are well-known to be highly reactive and involved in many biological processes.[1] Often the charge—i.e., the seed of reactivity—is transferred over long distances, as for example in photosynthesis. In early models, charge transfer (CT) was described as a superexchange process in which an electron donor and an electron acceptor are coupled by the orbitals of the intermediate molecular moiety, the bridge.[2−4] In this model the charge tunnels and has essentially no residence time in the bridge. Many recent investigations carried out at CT model systems,[5−7] peptides[8−17] and DNA strands[18−22] focus on the question to which extent bridge sites are involved in the CT as intermediate charge positions. In the meantime "superexchange" and "charge hopping" are coexisting models and the question which concept has to be applied depends on the relative donor-bridge-acceptor energetics. Clearly the model of charge hopping through several sites applies if it is energetically possible to inject the charge into the bridge. For example, in photoactivated peptide radical cations, the charge can use the chromophore, the peptide bond sites or the N terminal as steps for charge migration.[8,9] Whereas the charge hopping in peptide cations in the gas-phase had model character, this mechanism is now well accepted for DNA in solution.[18−22]

For neighboring amino acids in peptides the energetics of the sites "charge in the peptide bond *i*" and "charge in the peptide bond $i + 1$" is in a zeroth order picture given by the local ionization energy (IE) of the CO−NH group modified by the amino acid side chains.[9] In the case of peptides consisting of glycyl, alanyl, and leucyl the local IEs of the peptide bonds are very similar and lie in the range of 9.0 to 9.3 eV.[9] Other amino acids are also expected to exhibit similar IEs in the peptide bond. Only the IEs of the amino groups at the N terminal (8.5−8.8 eV, depending on the specific amino acid at the N terminal) and of aromatic chromophores (7.4−8.4 eV depending on the chromophore) lie at lower energies.[9] It is therefore evident that along an arbitrary peptide chain the charge has to go through (a) isoenergetic, (b) uphill, and (c) downhill steps.

In the case of two isoenergetic or energetically similar neighboring charge sites a strong coupling, a mixing of the local to global states, and a splitting of the global states is expected. In this case charge motion would take place on an electronic time scale ($\tau < 20$ fs[4]) and is experimentally observed as a static charge delocalization.[6] This concept has been applied by Remacle, Levine, and co-workers to calculate ultrafast multisite CT through peptides.[10−12] Here the CT is faster than any vibration and is assumed to directly couple into a fast dissociation channel. The time scale of the electron motion is expected to slow considerably down with decreasing inter-site coup-

* To whom correspondence should be addressed.
† TU München.
‡ Present address: Accenture GmbH, Maximilianstrasse 35, D-80539 München.
§ Heinrich-Heine-Universität.

10.1021/jp0210935 CCC: $30.25
Published on Web 08/20/2005

ling,[4,10−12] i.e., with increasing energy difference or distance between the two charge sites.

The time scale for an uphill CT should depend on the internal vibrational energy and the energetics of the electronic states. The following cases can be distinguished: (i) the electronic coupling is strong enough to allow a fast transfer through the barrier,[10−12] (ii) the vibrational energy is reconverted into electronic energy by a statistical process, or (iii) the jump to the higher electronic surface is initiated by a surface hopping initiated by an internal rotation.[14−17] Obviously for the peptide systems investigated in ref 9 at low internal energies electronic uphill steps are slow in comparison to the nanosecond laser pulses used, favoring explanation ii.

The literature on downhill CT in cations in the gas phase is sparse. Jortner et al. proposed that in the gas-phase CT should be described as internal conversion (IC).[23,24] For small energy gaps between the electronic states IC is predicted to be very fast.[25] Levy and co-workers investigated CT in various isolated cationic donor-bridge-acceptor systems and found a CT dynamics much faster than their nanosecond laser pulses.[26] In this work, a local resonant two-photon ionization (R2PI) in the chromophore with the higher IE, was assumed.

The local ionization in phenylethyl-*N*,*N*-dimethylamine (PENNA), into the energetically higher charge site is supported by the observation of dissociation directly after ionization[7] and has been proven by photoelectron (PE) spectroscopy.[27] The PE spectra show that R2PI through the origin of S_1 of the phenyl moiety forms PENNA ions preferentially in the excited cation state "charge in the phenyl site". The fact that the PE spectra do not show vibrational resolution is attributed to a short lifetime of this state due to fast CT. The extension of the PE intensity down to energies below the expected IE of the phenyl moiety is tentatively assigned to a vibronic coupling and an intensity borrowing of highly excited vibrations of the state "charge at the amine site" to the first excited cation state "charge at the phenyl site". This intensity borrowing leads to a situation where not all of the PENNA ions (but still more than 50%) are formed in the state "charge in the phenyl moiety".

In this paper we report on femtosecond (fs) pump−probe experiments on the downhill CT in PENNA. The R2PI by an ultraviolet (UV) femtosecond laser pulse is the pump and resonant multiphoton photofragmentation by a visible (vis) femtosecond laser pulse the probe excitation. The intensity of the fragment in dependence of the pump−probe delay provides the time scale of the CT. The relevance of several models for the CT in PENNA is discussed.

II. Experimental Section

Two different setups have been used to record R2PI spectra of PENNA and probe the transient presence of the charge at the phenyl chromophore site with nanosecond and femtosecond laser pulses. The nanosecond (ns) R2PI spectra have been recorded in a reflectron time-of-flight mass spectrometer (RETOF-MS),[7] which also allows detection of metastable fragmentation processes.[28] The nanosecond experiments were performed with two conventional tunable narrow-bandwidth excimer-pumped dye lasers (Lambda Physics). The laser pulse width was 5 ns in the UV and 7 ns in the vis. The laser output energy was typically 10 μJ (pulse energy range tested: 5−50 μJ) per pulse in the UV and 2 mJ in the vis. The lens for focusing into the RETOF ion source had a focal length of 300 mm. The focus diameters were about 600 μm for the UV and the vis wavelength. A typical repetition rate was 10 Hz.

The second experimental setup combines a femtosecond laser system with a linear TOF-MS[29] with second-order space focus.[30] This apparatus consists of three vacuum chambers. The first contains the inlet valve and the skimmer, the second the ion source and the third drift tube and detector. The pulsed inlet valve has an orifice of 150 μm and could be heated to 500 K. The sample bottle is mounted inside the vacuum chamber and heated together with the valve. The nozzle Ar backing pressure was 1 bar. Unfortunately the nozzle could only be operated at a repetition rate of 125 Hz, which limited considerably the data acquisition rate. To achieve collision-free conditions a 0.95 m^3/s turbo molecular pump evacuates the inlet chamber. The molecular beam is skimmed 40 mm downstream with a heated skimmer with a 1 mm diameter orifice. The neutrals drifted into the second vacuum chamber and into the deflection plate assembly of the ion source. In the middle of the first field of the two-stage ion source the molecular beam was perpendicularly crossed by the laser pulse. Ions were formed by a UV R2PI. They were extracted perpendicular to the molecular beam and the laser into the third chamber and to the ion detector by a 1300 V pulse applied at the repeller plate. The two-field ion source was constructed in such a way that the space focus could be corrected to the second order and projected onto the detector.[29] The flight path was 50 cm and the mass resolution $m/\Delta m = 750$. When recording the full mass spectrum an oscilloscope with a transient digitalization rate of 100 megasamples per second was used so that mass spectra of 20 μs flight time were recorded with 1 ns accuracy. This time resolution for data acquisition did not affect the mass resolution of the TOF-MS, but the data acquisition rate was reduced to 30 Hz. Therefore, to profit from the full repetition rate of the pulsed valve we used boxcar integrators to record the pump−probe spectra.

The femtosecond laser was a commercially available system consisting of a Ti:Sappire oscillator (Coherent Mira Basic), a regenerative amplifier (Spectra Physics Super-Spitfire) followed by a multipass amplifier, both pumped by the second harmonics of a kHz Nd:YLF Laser (Spectra Physics Super-Merlin). The pulses of the fundamental of the Ti:sapphire had a duration of 80 fs, a wavelength of 790 nm and a pulse energy of 2 mJ. The laser pulse was then split into two beams of equal energy. One was delayed against the other by a computer-controlled optical delay. Both beams were frequency-converted by parametric generators (Light Conversion TOPAS) into tunable IR radiation which then was mixed with the fundamental of the Ti:sapphire laser into a green wavelength range. One of the two green laser pulses was used for probe detection (vis). The other was frequency-doubled to create the UV pump laser pulses. The pump laser wavelength was tunable between 230 and 280 nm with a typical pulse energy of 5 μJ. The pulse duration in the UV was 200 fs as measured directly in the supersonic expansion via nonresonant two-photon ionization of furan. The error in the zero delay was 20 fs. The vis probe laser wavelength was tunable between 460 and 560 nm with a pulse energy of about 30 μJ and a pulse width of 120 fs. The laser pulses were slightly focused to the target with a 500 mm lens (out of focus, focus diameter about 4 mm for UV and vis). Note that despite the very different laser pulse lengths the intensities of the nanosecond and femtosecond laser pulses were chosen to be as similar as possible: nanosecond UV, $I \sim 3.6 \times 10^6$ W/cm^2 or lower;[7] femtosecond UV, $I \sim 8 \times 10^7$ W/cm^2; nanosecond vis, $I \sim 1 \times 10^8$ W/cm^2; femtosecond vis, $I \sim 2 \times 10^9$ W/cm^2. To achieve this and still have enough signal-to-noise ratio for the femtosecond experiment a larger focal size and a higher repetition rate than in the nanosecond experiment was used.

III. Results and Discussion

In the following sections, we present R2PI spectra of PENNA recorded by tuning nanosecond and femtosecond lasers (III.1) and monitor the CT dynamics by nanosecond and femtosecond laser pulse pump−probe excitations (III.2).

III.1. Local Ionization of PENNA with Femtosecond Laser Pulses. A precondition for the observation of ultrafast CT in PENNA cations is that the charge can be initially localized in the phenyl moiety (pump excitation). In the case of PENNA such local ionization can be achieved with nanosecond laser pulses by R2PI through the local S_1 of the phenyl chromophore.[7] Due to the shorter pulses in femtosecond compared to nanosecond experiments typically much higher intensities are used in femtosecond laser pulse experiments. At high-intensity new absorption channels with low excitation cross sections may be addressed. Such channels are (i) near-resonant ionization at the phenyl site, (ii) nonresonant ionization at the amine site or (iii) three-photon ionization via super-excited states.[31,32] The presence of (ii) has been even observed in femtosecond PE spectra recorded at very low laser intensities (repetition rate: 50 kHz).[27] The same experiment also showed that three photon ionization via super-excited states (iii) does not occur in PENNA.

The best way to reduce the effects (i) and (ii) are low femtosecond laser pulse energies. Despite the very different laser pulse lengths of 5 ns vs 200 fs we tried to keep the intensities as similar as possible. The intensity in the nanosecond UV laser pulse was 3.6×10^6 W/cm^2 and the intensity in the femtosecond UV laser pulse 8×10^7 W/cm^2. To obtain a good signal-to-noise ratio in the femtosecond laser experiment, we used a relatively high repetition rate of 125 Hz (nanosecond laser experiment:[7] 10 Hz) and a very large laser molecule interaction volume which allowed to address more molecules than in the nanosecond experiment.

The best argument we have to exclude strong contributions of (ii) is the similarity of the femtosecond R2PI spectrum (Figure 2a) with the nanosecond R2PI spectrum (Figure 2b): The femtosecond R2PI spectrum contains essentially the same resonances with similar intensities as the nanosecond laser R2PI. This shows that in the femtosecond experiment we are still predominantly exciting at the phenyl chromophore. To our knowledge this is the first frequency scanned UV spectrum with a femtosecond laser. Because of the strong fragmentation directly after ionization we measured the R2PI spectrum of PENNA by recording the fragment ion mass 58 Da (fragment $(CH_3)_2N^+ = CH_2$, see also Figure 1a) in dependence on the laser wavelength (for a detailed explanation see ref 7). The spectrum was attributed to the intact PENNA species because of the energetic position of the S_1 and its vibrational fingerprint.[7] The nanosecond laser R2PI spectrum (Figure 2b) is sharp, which is in agreement with the expected nanosecond lifetime of the phenyl S_1 state. With the help of theory the spectrum is attributed to the extended nonsymmetric anti conformer.[7]

The broadening of the femtosecond R2PI spectrum (Figure 2a) is mostly given by the bandwidth of the femtosecond laser of about 200 cm^{-1}. Some contribution of power-broadening seems to be also present. The relative and absolute nanosecond versus femtosecond intensities are similar. Also the peak positions of the femtosecond R2PI spectrum (Figure 2a) are within the resolution of the femtosecond laser in good agreement with the corresponding nanosecond R2PI spectra. No important new features are contained in the femtosecond R2PI spectrum. The small features at the low-energy edge of the S_0-S_1 origin transition might be due to hot bands. The presence of some vibrational excited molecules in the beam in the femtosecond but not in the nanosecond laser pulse experiment can be explained by the lower nozzle Ar backing pressure used in the

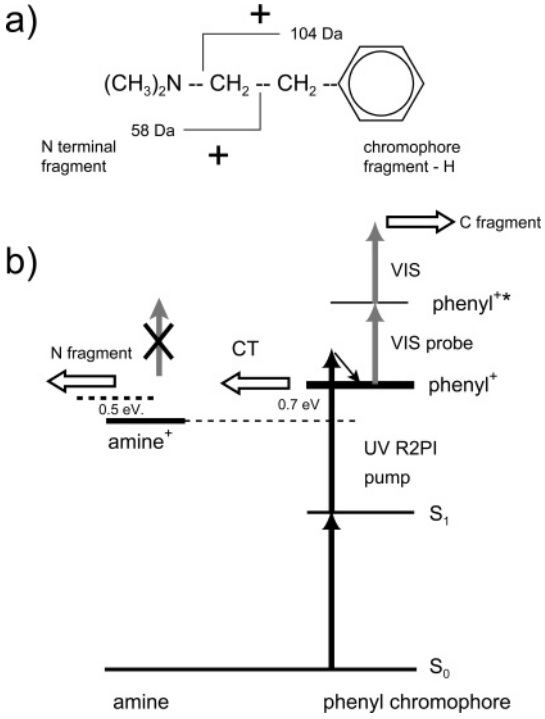

Figure 1. (a) Schematic structure of PENNA. Indicated are the lowest-energetic N terminal fragmentation channel (mass 58 Da) which opens directly after ionization and the chromophore ion fragmentation channel (mass 104) which only opens after excitation with multiple visible photons (see b). Note that formation of mass 104 needs a neutral H transfer to the amine and a reorganization. (b) Scheme of the resonant UV R2PI (pump excitation) and the cation photofragmentation (probe excitation). After local ionization at the phenyl chromophore (pump), the molecule can undergo CT to the amine site and subsequent fragmentation to the immonium cation is observed (mass: 58 Da). Resonant photoexcitation by vis probe photons, leading to the C fragment (mass: 104 Da), is only possible for a positively charged phenyl chromophore. When CT to the amine group is completed vis probe photons are not resonant with PENNA. As a result, the chromophore fragment ion intensity is a signature of the vis photoabsorption and the presence of charge in the phenyl chromophore.

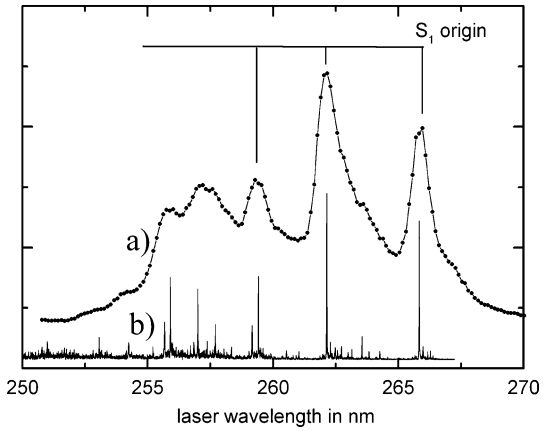

Figure 2. R2PI femtosecond (a, −●−) and nanosecond (b, −) multiphoton ionization spectra of PENNA. The R2PI spectra were recorded by using the amine fragment ion (mass: 58 Da) (for explanation see text and ref 7). The femtosecond laser R2PI spectrum is broader than the nanosecond spectrum because of the femtosecond laser bandwidth of 200 cm^{-1}.The main resonances of the phenyl chromophore are also found in the femtosecond R2PI spectrum. This proves the local character of the resonant femtosecond excitation. For further explanation, see text.

femtosecond setup. The fact that the femtosecond laser pulse R2PI spectrum does not reach the zero line between the first two transitions could be due to hot band transitions but also due to near-resonant excitation in phenyl. Small contribution of a nonresonant amine excitation as observed in femtosecond R2PI PE experiments cannot be excluded.

In conclusion, the femtosecond laser pulse R2PI spectrum is a control for the experimental conditions in the femtosecond laser pulse experiment and the local excitation at the phenyl site. Under our conditions nanosecond and femtosecond excitation behave similar except that femtosecond excitation is broad and contains some contribution of quasi-resonant excitation. There is no reason to doubt that most of the femtosecond laser excitation of PENNA is resonant at the phenyl chromophore and that ionization is local at this site.

III.2. Time Scale of the Charge Transfer in PENNA Cations.

III.2.A. Probing the Charge in the Phenyl Moiety with Nanosecond Lasers. Not knowing the time scale of the CT, we first investigated PENNA cations by nanosecond lasers. The experimental setup was the same used in ref 7. PENNA can be locally ionized at the phenyl chromophore by R2PI through the origin of the S_1 state (265.9 nm).[7,27] (right side, Figure 1b). After local ionization CT occurs. In this process electronic energy is converted to vibrational energy and most of the parent ions undergo metastable fragmentation.[7] The delayed-formed fragment ions can be directly observed in a RETOF mass spectrometer as a broad peak.[7] This metastable peak is expected to disappear if the cation would be photoexcited to several eV of internal energy: Upon excitation we expect a switch from a metastable decay on a μs time scale to a decay faster than 100 ns.

Green light (vis) can be efficiently absorbed by charged benzene,[33] benzene derivatives,[9,34,35] other aromatic molecules,[36,37] 2-phenylethylamine[38] and peptides containing phenylalanine.[9] Its therefore reasonable to assume that green light is also absorbed in the cationic phenyl group of PENNA. In addition the vis photoexcitation is nonresonant in neutral phenyl and the neutral and cationic amine.[37]

Using this information, we tried to "accelerate" the metastable decay by cation photoexcitation of PENNA with intense nanosecond light pulses with wavelengths of 530 nm, 520 nm, 510 and 500 nm (2 mJ pulse energy, 7 ns pulse width, intensity 1×10^8 W/cm^2). The ionization laser and the vis laser were synchronized to a perfect time overlap with an accuracy of 1 ns. The spatial overlap between the UV and the vis lasers and the photo fragmentation was tested and adjusted with benzene[33] each time before and after an experiment with PENNA.

At all wavelengths which we used no change of the intensity of the metastable decay peak was observed and no new fragment found. This result implies that the expected efficient phenyl cation vis absorption does not take place. Obviously in the cation the optical pumping rate of the nanosecond laser is much smaller than the rate for the CT from the phenyl to the amine site. A crude estimation with transition moments of benzene derivatives shows hat the CT in PENNA should be much faster than 50 ps to explain the nanosecond laser pulse result.

III.2.B. Pump−Probe Experiments with Femtosecond Laser Pulses. To follow the fast CT in PENNA radical cations, femtosecond pump−probe measurements were carried out. The excitation and dissociation scheme is the same as for the nanosecond laser experiment in section III.2.A (Figure 1b). For local ionization, the femtosecond UV laser was set to the S_0−S_1 origin transition of PENNA at 265.9 nm (pump excitation). The cation CT rate was probed by resonant femtosecond vis photoabsorption of the cation which was detected by the intensity of a photofragment which only appears at high internal energies. This is in total a UV R2PI ionization (pump) and a delayed resonant multiphoton photon vis cation excitation (probe). To our knowledge, this is the first pump probe experiment with this excitation scheme.

Fs probe wavelengths of 500, 505, and 510 nm were chosen because (i) at these wavelengths a high absorption cross section in the phenyl group of the PENNA cation is expected and (ii) the vibrational state density in the electronically excited phenyl state should be high enough so that the broad femtosecond vis laser is always resonant. The results of all three wavelengths were very similar, and we therefore only show the results achieved with the probe laser wavelength of 500 nm.

For PENNA the detection of the probe excitation by photodissociation is complicated because dissociation at the amine site occurs directly after ionization.[7] As in the nanosecond experiment, we tried to accelerate the metastable amine decay by the vis femtosecond laser excitation. This experiment failed, however, because the linear TOF-MS which we used for the femtosecond experiment is not suited for metastable decay detection.

Resonant multiphoton dissociation spectroscopy proved to be a valuable tool for cation excited-state spectroscopy.[33,34,39−41] Here the cation is resonantly excited by two or more photons. The first step is the resonant excitation and the other n photons serve for detection by fragmentation. The advantage of such a $1 + n$ multiphoton approach is that high-energetic dissociation channels are accessible, leading to new fragment ions. The appearance of such a new fragment is then directly correlated with the vis probe excitation.

In the case of PENNA the fragment of mass 104 Da was intense enough to record a pump−probe spectrum with a good signal-to-noise ratio. In the following we term this fragment ion "C fragment". A hydrogen transfer to the amine is necessary to create the ion with mass 104 Da (see Figure 1a, right side) and the neutral dimethylamine. The positively charged phenyl fragment is then stabilized by isomerization to phenyl-ethylene. The vis probe laser pulse alone formed no PENNA cations and fragments.

III.3. The Expected Pump—Probe CT Signal and Other Interfering Signals. As explained above the signal of interest is the intensity of the fragment ion of mass 104 Da as a function of the UV pump pulse and vis probe pulse delay. Because of the resonant intermediate step for the pump excitation, the pump−probe excitation scheme is more complicated in comparison to usual one-photon pump and one-photon probe femtosecond excitations. In parts a−c of Figure 3, the fragment ion signals and the excitation schemes of resonant and nonresonant UV−vis pump probe laser pulse excitations of PENNA are schematically displayed.

In Figure 3a, the UV−vis pump−probe excitation scheme monitoring the PENNA cation CT dynamics is shown for different CT times. Assuming an infinite lifetime of the state with the charge in the aromatic chromophore ($k_{CT} = 0$) the vis absorption of the chromophore and hence the C fragment intensity is expected to rise at $t = 0$ and then stay constant at all positive delays (trace i). For a small CT rate, a decay of the fragment ion signal at longer delay times is expected (trace ii). Here the rise and the fall rates are nearly independent. For a CT time faster than or comparable to the femtosecond laser pulse widths a clear separation between the cation build up time and the CT time is complicated (Figure 3a, trace iii).

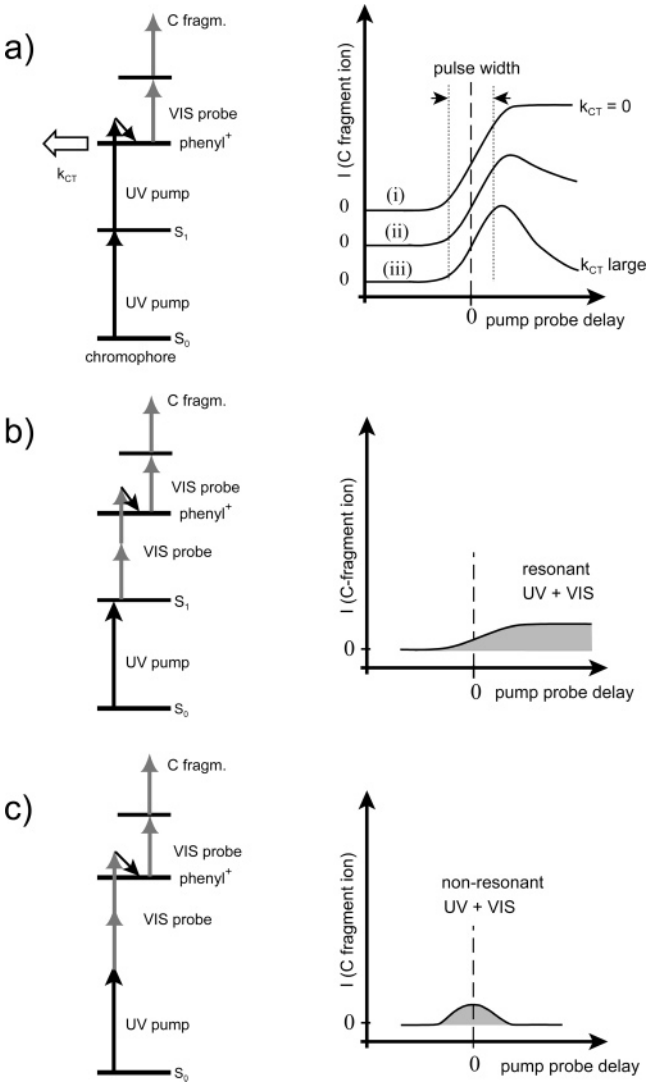

Figure 3. Pump-probe CT signal (a) and interfering signals (b, c) caused by the complex two color multiphoton pump probe excitation scheme. (a) UV−vis pump−probe excitation scheme is shown which is suitable to monitor the transient charge population in the chromophore. For $k_{CT} = 0\ s^{-1}$ after an induction time, the chromophore absorption and hence the chromophore fragmentation is expected to stay constant (trace i). For a medium charge decay rate the fragment ion signal is expected to decrease at longer times (trace ii). For an ultrashort decay of the charge in the phenyl moiety the decay rate also affects the rising slope of the signal. (b) After UV excitation, the remaining S_1 population can be ionized by two photons of the intense vis probe laser. Because of the ns lifetime in S_1 this is also possible for very long pump−probe delays. As a result the parent ion intensity is increased at positive pump probe delays by a small constant, contribution. The ions which were formed during the vis laser pulse can be also be further photofragmented by the same pulse (see gray socket in the fragment ion signal). This fragmentation is then due to the 1·UV pump $(2 + 1 + n)$·vis probe excitation scheme probing the neutral S_1 dynamics of PENNA. (c) During the overlap of pump and probe pulses in addition nonresonant (at the amine site) or quasi-resonant (at the phenyl site) process are possible which enhance the parent ion formation and hence equally the fragment ion formation.

Beside the signal of interest (Figure 3a, case iii), the vis probe laser pulse can also ionize the population left in S_1 by the UV pump laser (Figure 3b). This is a 1·UV pump 2·vis probe scheme, reflecting the neutral S_1 dynamics. Note that this dynamics is directly found in the parent ion signal and also in the C fragment ion signal and does not carry the information on the CT dynamics (Figure 3b). Usually one would try to separate the pump−probe process from background signals by a difference measurement. This is, however, not possible here because the process of a UV S_1 excitation followed by a two-photon vis ionization and a subsequent $1 + n$·vis dissociation (same laser vis pulse) is clearly also caused by the pump and probe laser pulses, as is the signal of interest.

During the overlap of pump and probe pulses also nonresonant (at the amine site) or quasi-resonant (at the phenyl site) UV−vis processes can happen (Figure 3c). This coherent pump−probe signal is symmetric around the delay time $t = 0$ like a cross-correlation of the two laser pulses (Figure 3c). It enhances parent cation and hence also fragment ion formation equally. The problem of non- or quasi-resonant ionization processes is for PENNA more severe than in usual femtosecond experiments, because we have a severe mismatch between our sharp S_1 structures (Figure 2b) and the large bandwidth of the UV femtosecond laser light (see width of the femtosecond R2PI spectrum in Figure 2a). In a simplified explanation, most of the ionization takes place by photons which are not perfectly resonant with S_1, but which still can be used for ionization because of the artificial lifetime broadening of S_1 by the short laser pulse excitation. As a consequence, the ionization and also the photofragmentation efficiencies increase during the overlap of the UV and vis laser pulses.

III.4. The Experimental Parent Cation Signal. Usually the UV R2PI pump excitation produces a constant parent cation signal, which is independent of pump−probe delay. This is not the case here because of processes b and c in Figure 3. In Figure 4a, the measured sum of the parent and the N fragment cation pump−probe signal is displayed (sum of the intensities of the masses 149 and 58 Da) because the N fragment decay is slow and during the probe excitation the N fragments were not yet formed. Therefore, the number of intact molecules at the time of the probe laser access is the sum of the N fragment and the parent cation intensities.

As outlined above, beside the constant ion contribution by the femtosecond UV R2PI (dashed line, please note the position of the zero label at the *y* axis) also other time-dependent contributions exist. The resonant UV−vis ionization with S_1 as an intermediate storage level and the nonresonant or quasi-resonant UV−vis ionization. The resonant UV−vis ionization signal reaches its maximum after the UV laser pulse is off and the S_1 population is maximized (compare Figure 3b and Figure 4a, right side) and should stay constant because of the long lifetime of the S_1 state of PENNA. For PENNA this process adds about 10% signal to the parent ion signal. The nonresonant UV−vis ionization signal is found around zero delay (compare Figure 4a at pump−probe delay = 0 to Figure 3c). It causes about 30% increase of the cation signal. The line curve in Figure 4a corresponds to a two-level model simulation with suitable optical pumping rates.

III.5. The Experimental Chromophore Fragment Ion Signal. Figure 4b shows the ion signal of the C fragment ion (mass: 104 Da) in dependence of the pump−probe delay. It shows a steep rise close to zero pump−probe delay and then a delayed decay. The rise can be explained by the fact that fragment ions can only be formed by the probe laser after ions were first produced by the pump laser (Figure 3a). In case that charge transfer would not take place one would expect a strong constant *C* fragment signal (see dashed line in Figure 4b). The lack of this strong constant signal shows that although parent cations are present they are no longer available for the femtosecond vis probe excitation, a clear indication for the CT process.

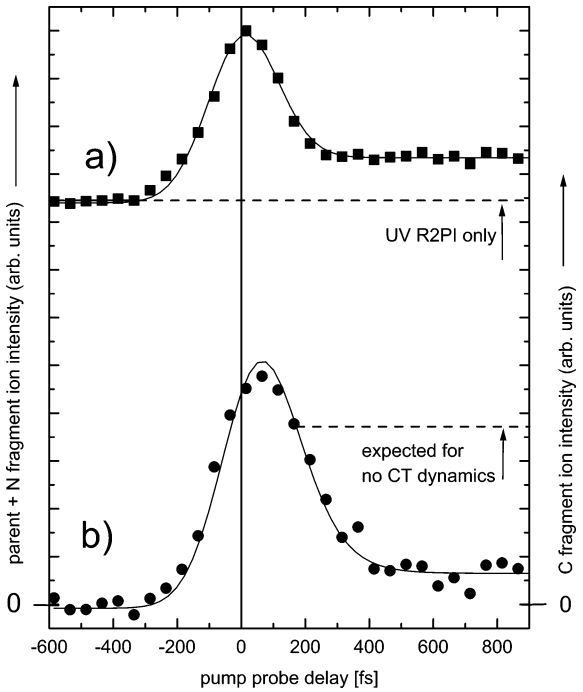

Figure 4. (a) Femtosecond pump−probe spectrum (−■−) recorded by detection of the sum of the parent and the N fragment ions. Note that the parent cation decay is metastable and that at the time of the probe pulse still all ions are PENNA parent cations. Note the large time-independent ion signal, which is due to the UV R2PI signal. This signal is present at all times especially also at positive delays (see dashed line). Clearly the spectrum also contains time-dependent contributions. They are due to (i) resonant and (iii) non- or quasi-resonant UV−vis processes as explained in Figure 3, parts b and c. The fit of a two-level system model is shown as line graph. b) Femtosecond pump−probe spectrum (−●−) recorded by detection of the phenylethylene fragment ion (C fragment: mass 104 Da). After a steep rise around zero delay, we observe a fast delayed decay. The decay occurs although still intact parent cations are present (see a) and is interpreted as a signature of the charge transfer from the phenyl chromophore to the amine group. The delay of the onset can be explained by the fact that fragment ions can be only formed by the probe laser after first parent ions were formed by the pump laser (see Figure 3a). At large delays a small constant background signal is present. This is explained by a $1{\cdot}UV + 2{\cdot}vis$ ionization and a subsequent $1 + n{\cdot}vis$ photofragmentation (Figure 3b). The nonresonant UV−vis ionization (Figure 3c) contributes less than 30% to the fragment ion signal and is symmetric to the zero delay. It cannot account for the shift of the signal to longer pump−probe delays. On the basis of two coupled two-state models the best fit (see line graph) gives a lifetime of the state "charge in the phenyl chromophore" of $\tau_{CT} = 80 \pm 28$ fs.

At longer pump−probe delays still some photofragments are observed despite the fact that the CT is over. This signal is attributed to the resonant two-color UV-2vis ionization process (Figure 3b) where the vis laser forms PENNA ions which then can be fragmented by the same vis laser pulse.

As mentioned above, in the C fragment ion signal also the "overshooting" by nonresonant or quasi-resonant UV−vis ionization (see Figure 3c) is contained. For the parent PENNA cation this contribution is 30%. For the C fragment, this contribution should be less than that. The nonresonant signal is symmetric about the delay time zero and cannot account for shift of the signal to longer pump−probe delays.

In Figure 4b, also a fit on the basis of two coupled two-level models (UV−vis ionization and UV ionization and vis dissociation) is shown (solid line graph), which takes both resonant and nonresonant contributions into account. An exact mathematical analysis of this fit results in a CT rate of $\tau_{CT} = 80 \pm 10$ fs. A sensitivity analysis shows that a high accuracy of the zero delay is essential to obtain a reliable CT rate. In this experiment the zero-delay was calibrated by simultaneous nonresonant ionization of co-expanded furan. Nevertheless a remaining inaccuracy of the zero-delay of 20 fs remains, which is due to statistical ion intensity fluctuations and the pump−probe delay step resolution. This zero delay time error causes a total error of 28 fs.

III.6. The Mechanism of Charge Transfer in PENNA. We explain the time-dependent change of the absorption cross section for vis light of the parent cation of PENNA by a CT process. With the help of theory for neutral PENNA it was previously possible to identify the thermally most populated structure as an extended anti conformer.[7] Hence we attribute the observed dynamics of 80 ± 28 fs to the CT from the phenyl chromophore through a $-CH_2-CH_2-$ bridge to the methylated amine group. Unfortunately we were not able to control the internal energy of the cation directly after ionization. The maximum ionization excess energy was 0.6 eV but most of the energy could be taken away by the leaving electron as observed in PES.[27] To obtain more detailed information about the mechanism it would be extremely helpful to record the CT rate as a function of internal energy.

From our data we cannot directly extract a detailed mechanism. Nevertheless, because of the finite CT time we can exclude a direct electronic process without a contribution of nuclear motion. Three mechanisms may account for the observed CT dynamics of 80 ± 28 fs: (i) a conventional internal conversion process (IC), (ii) a conical intersection, or (iii) motion on a single electronic surface.

(i) The CT time of 80 ± 28 fs is fast, but could be still explained with a conventional IC between electronic states as proposed by Jortner and co-workers for downhill CT in the gas phase.[23,24] In this process the rate is given by the product of an electronic coupling factor and a factor considering the Franck−Condon overlap between the two states. On one hand the electronic coupling may be large due to the relative small energy difference of 0.7 eV of the two participating electronic states and the small bridge length.[2−4] On the other hand, a large Franck−Condon overlap is expected (see the energy gap rule[25]) because of the small energetic spacing and the different geometries of the two states especially at the amine site. A strong coupling as well as the expected large density weighted Franck−Condon factor would be suitable to explain an IC time scale of about 100 fs. For example Jortner and co-workers estimated the density weighted Franck−Condon factor to be 10^{-4} cm^{-1} for a model system with four vibrational modes ($\nu_1 = 200$ cm^{-1}, $\nu_2 = 500$ cm^{-1}, $\nu_3 = 1200$ cm^{-1}, $\nu_4 = 1500$ cm^{-1}) and a 0.9 eV energy gap.[25] This value and a relatively weak electronic coupling factor of 300 cm^{-1} would explain the observed rate. In this case the observed time scale would be presumably the time for changing the surface.

(ii) The small energetic distance and the geometry distortion between the two electronic states can also cause a conical intersection.[42] There are two coordinates which are candidates for conical intersections. The neutral amine group is pyramidal (double well potential) and the positively charged amine group would be planar (single well potential). Because the upper state has the broad double well structure a conical intersection with the single well ground state potential can happen. The same consideration holds for the rotation of the amine group. Whereas in the extended PENNA the methyl groups of the neutral amine site are twisted outward into a nonsymmetric position (note that this position is degenerate), in the cation ground state they are rotated into the symmetric position. This leads again to a double

well potential of the upper state and a single well potential in the lower state in the internal C−N rotational coordinate. In the case of a conical intersection, the observed time scale of the CT is presumably not the surface hopping time but the time to reach the conical intersection. More insight in the applicability of conical intersections for the CT in PENNA could be gained by theoretical investigations.

(iii) The third model would be a CT on a single electronic surface where different nuclear geometries correspond to different molecular charge distributions. Such a mechanism was observed for the excited state of $[I\cdot(H_2O)_n]^-$ ($n > 4$) clusters,[43] where the site and the size of the wave function of the charge was directly coupled to the nuclear motion of the solvent molecules. Until now there is, however, no indication for a similar behavior in extended flexible molecules.

Most of the fast and ultrafast S_2-S_1 radiation-less relaxation processes, which are the basis of Kasha's rule,[44,45] are explained by conventional IC or conical intersections. In principle both mechanisms can account for the fast CT time scale in PENNA, although a conical intersection might be more probable.

IV. Conclusion

In PENNA the two sites "charge in the phenyl chromophore" and "charge in the amine group" are energetically well separated and local. Because the state "charge in the phenyl chromophore" is the exited state of PENNA the charge can move to the lower-energetic amine site. The neutral and the photoexcited cation ground state conformers have been found by theoretical calculations to be extended[7] and the observed C*T* is therefore a "through-bond" CT. On the basis of our femtosecond pump−probe measurements, the decay time of the state "charge in the phenyl site" is 80 ± 28 fs. This CT time is not in the time domain expected for direct electronic processes and therefore nuclear motions should be involved. A detailed mechanism for the downhill CT between the two energetically close-lying electronic states cannot be derived from the CT rate only. Funneling through a conical intersection is favored but also conventional IC could explain the observed rate.

For radical cations with two charge sites spaced by a $-CH_2-CH_2-$ bridge in gas phase our experimental results give a first time scale for the downhill CT. This result might be transferable to similar CT processes with similar energetics in extended systems, such as in peptides or in DNA. One has to consider, however, that this ultrafast time scale is only expected for a downhill CT. Neither the time scale nor the mechanism is transferable to uphill CT steps or CT between isoenergetic sites.

For better understanding it would be helpful to conduct similar experiments at other molecular model systems with different energetics and inter-site distances as well as defined relative donor−acceptor orientations.

Acknowledgment. We acknowledge financial support of the Volkswagenstiftung within the framework of the Schwerpunkt "Intra- and intermolecular electron transfer".

References and Notes

(1) George, M.; Griffith, J. S. *The Enzymes I*; Academic Press: New York, **1959.**
(2) Halpert, J.; Orgel, L. E. *Discuss. Faraday Soc.* **1960**, *29*, 32.
(3) McConnel, H. M. *J. Chem. Phys.* **1961**, *35*, 508.
(4) Reimers, J. R.; Hush, N. S. *Chem. Phys.* **1989**, *134*, 323.
(5) Weinkauf, R.; Lehrer, F. *Resonance Ionization Spectroscopy*, Vickerman, J. C., Lyon, I., Lockyer, N. P., Parks, J. E., Eds.; The American Institute of Physics, Bristol, PA, 1998; p 117.
(6) Weinkauf, R.; Lehrer, F.; Schlag, E. W.; Metsala, A. *Discuss. Faraday Soc.* **2000**, *115*, 363.
(7) Weinkauf, R.; Lehr, L.; Metsala, A. *J. Phys. Chem. A* **2003**, *107*, 2787.
(8) Weinkauf, R.; Schanen, P.; Yang, D.; Soukara, S.; Schlag, E. W. *J. Phys. Chem.* **1995**, *99*, 11255.
(9) Weinkauf, R.; Schanen, P.; Metsala, A.; Schlag, E. W.; Bürgle, M.; Kessler, H. *J. Phys. Chem.* **1996**, *100*, 18567.
(10) Remacle, F.; Ratner, M. A.; Levine, R. D. *Chem. Phys. Lett.* **1998**, *285*, 25.
(11) Weinkauf, R.; Schlag, E. W.; Martinez, T.; Levine, R. D. *J. Phys. Chem.* **1997**, *101*, 7702.
(12) Remacle, F.; Levine, R. D.; Schlag, E. W.; Weinkauf, R. *J. Phys. Chem. A* **1999**, *103*, 10149.
(13) Schlag, E. W.; Lin, S. H.; Weinkauf, R.; Rentzepis, P. M. *Proc. Natl. Acad. Sci. US.A.* **1998**, *95*, 1358.
(14) Baranov, L. Ya.; Schlag, E. W. *Z. Naturforsch.* **1999**, *54a*, 387.
(15) Schlag, E. W.;. Sheu, S.-Y.; Yang, D.-Y.; Selzle, H. L.; Lin, S. H. *J. Phys. Chem. B* **2000**, *204*, 7790.
(16) Schlag, E. W.; Yang, D.-Y.; Sheu, S.-Y.; Selzle, H. L.; Lin, S. H.; Rentzepis, P. M. *Proc. Natl. Acad. Sci. U.S.A.* **2000**, *97*, 9849.
(17) Schlag, E. W.; Sheu, S.-Y.; Yang, D.-Y.; Selzle, H. L.; Lin, S. H. *Proc. Natl. Acad. Sci. U.S.A.* **2000**, *97*, 1068.
(18) Gasper, S. M.; Schuster, G. B. *J. Am. Chem. Soc.* **1997**, *119*, 12762.
(19) Jortner, J.; Bixon, M.; Langenbacher, T.; Michel-Beyerle, M. E. *J. Am. Chem. Soc.* **1998**, *120*, 12950.
(20) Meggers, E.; Michel-Beyerle, M. E.; Giese, B. *J. Am. Chem. Soc.* **1998**, *120*, 12950.
(21) Giese, B.; Wessely, S.; Spormann, M.; Lindemann, U.; Meggers, E.; Michel-Beyerle, M. E. *Angew. Chem.*. **1999**, *38*, 996.
(22) Henderson, P. T.; Jones, D.; Hampikian, G.; Kan, Y.; Schuster, G. B. *Proc. Natl. Acad. Sci. U.S.A.* **1999**, *96*, 8353.
(23) Jortner, J.; Bixon, M.; Heitele, H.; Michel-Beyerle, M. E. *Chem. Phys. Lett.* **1992**, *157*, 197.
(24) Jortner, J.; Bixon, M.; Wegewijs, B.; Verhoeven, J. W.; Rettschnick, R. P. H. *Chem. Phys. Lett.* **1993**, *205*, 451.
(25) Engelman, R.; Jortner, J. *Mol. Phys.* **1970**, *18*, 145.
(26) Cattoraj, M.; Laursen, S. I.; Paulson, B.; Chung, D. D.; Closs, G. L.; Levy, D. H. *J. Phys. Chem.* **1992**, *96*, 8778.
(27) Cheng, W.; Kuthirummal, N.; Gosselin, J.; Sølling, T. I.; Weinkauf, R.; Weber P. M. *J. Phys. Chem. A* **2005**, *109*, 1920.
(28) Kühlewind, H.; Boesl, U.; Weinkauf, R.; Neusser, H. J.; Schlag, E. W. *Laser Chem.* **1983**, *3*, 3.
(29) Lehr, L.; Weinkauf, R.; Schlag, E. W. *Int. J. Mass Spectrom.* **2001**, *206*, 191.
(30) Weinkauf, R.; Walter, K.; Weikhardt, C.; Boesl, U.; Schlag, E. W. *Z. Naturforsch.* **1989**, *44a*, 1219.
(31) Schick, C. P.; Weber, P. M. *J. Phys. Chem. A* **2001**, *105*, 3725.
(32) Schick, C. P.; Weber, P. M. *J. Phys. Chem. A* **2001**, *105*, 3735.
(33) Walter, K.; Weinkauf, R.; Boesl, U.; Schlag, E. W. *Chem. Phys. Lett.* **1989**, *155*, 8.
(34) Walter, K.; Boesl, U.; Schlag, E. W. *Chem. Phys. Lett.* **1989**, *162*, 261.
(35) Ripoche, X.; Dimicoli, I.; LeCalve, J.; Piuzzi, F.; Botter, R. *Chem. Phys.* **1988**, *124*, 305.
(36) Inokichi, Y.; Ohashi, K.; Matsumoto, M.; Nishi, N. *Laser Chem.* **1995**, *99*, 3416.
(37) Kimura, K.; Katsumata, S.; Achiba, S.; Yamazaki, T.; Iwata, S. *Handbook of HeI Photoelectron Spectra of Fundamental Organic Molecules*; Japan Scientific Press: Tokyo, 1980.
(38) Weinkauf, R.; Lehr, L. Unpublished results.
(39) Weinkauf, R.; Walter, K.; Boesl, U.; Schlag, E. W. *Chem. Phys. Lett.* **1987**, *141*, 267.
(40) Walter, K.; Weinkauf, R.; Boesl, U.; Schlag, E. W. *J. Chem. Phys.* **1988**, *89*, 1914.
(41) Cha, Ch.; Weinkauf, R.; Boesl, U. *J. Chem. Phys.* **1995**, *1023*, 5224.
(42) Domcke, W.; Stock, G. *Adv. Chem. Phys.* **1997**, *100*, 1.
(43) Lehr, L.; Zanni, M. T.; Frischkorn, C.; Weinkauf, R.; Neumark, D. M. *Science* **1999**, *284*, 635.
(44) Kasha, M. *Discuss. Faraday Soc.* **1950**, *9*, 14.
(45) Birks, J. B. *Organic Molecular Photophysics*; Wiley & Sons Inc.: Bristol, U.K., 1973; Vols. I and II.